Proceedings of MPT2009-Sendai
JSME International Conference on Motion and Power Transmissions
May 13-15, 2009, Matsushima IslesResort, Japan

MPT-03

Design of Nonlinearity of Passive Stiffness using Closed Kinematic Chain for Impact Absorption

*Masafumi OKADA† and Jun TAKEISHI‡

†*Dept. of Mechanical Sciences and Engineering, Tokyo TECH*
‡*Dept. of Mechanical and Intelligent Systems Engineering, Tokyo TECH*
2-12-1 Oookayama Meguro-ku Tokyo, 152-8552, Japan
e-mail : okada@mep.titech.ac.jp

Keywords : passive stiffness, nonlinearity design, closed kinematic chain, impact absorption

Abstract

Realization of mechanical softness is an important issue for a safe and adaptive control of robots in the real world. However, because the robot also requires stiffness for task execution, the simultaneous realization of softness and stiffness is necessary. In this paper, we design a nonlinear passive stiffness using closed kinematic chain. Because the proposed mechanism utilizes linear spring and nonlinearity of the closed kinematic chain, we can easily design the nonlinearity of the stiffness by changing the link parameters of members. The proposed mechanism is used for the leg of a robot and the mechanical parameters (length of members) are optimized so that the impact force on landing is reduced. The effectiveness of the proposed mechanism and optimization method are evaluated by simulations.

1 Introduction

Mechanical softness of robot members and/or joints is an important issue for safety and adaptation to its environments points of view in the real world. As shown in figure 1, the softness absorbs the impact force in the collision with humans and prevents from a breakage by itself. From this consideration, some researchers have developed the softness of robots so far, which are widely classified into the following three categories.

(1) Active compliance / impedance control realizes a virtual spring and damping by a torque and force control of actuators [1]∼[5]. This method is effective because an arbitrary characteristic of compliance or viscosity will be realized, however, does not deal with the instantaneous impact force because of the latency of the closed loop bandwidth of control. Moreover, the controller will be complicate and sometimes unstabilizes the robot system (appropriate control parametrs are required).

(2) Passive compliance is realized by mechanical softness. This method has high reliability and robustness, however, low adaptability becase its complaint characteristic is fixed and limited. To overcome this problem, nonlinearity of the stiff-

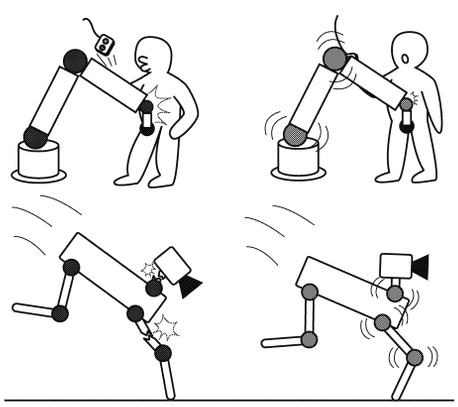

Figure 1: Impact absorption with elastic joints

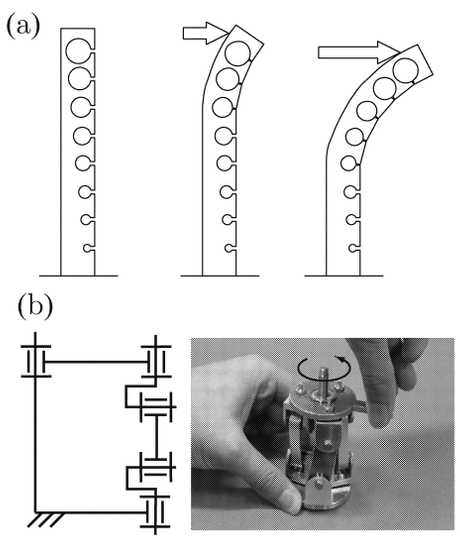

Figure 2: Nonlinear spring

ness is introduced. For example, we have developed a nonlinear elastic link as shown in figure 2-(a) [6] and a torque transmissioin mechanism using singulality of the closed kinematic chain as shown in figure 2-(b) [7]. These mechanisms realize high nonlinearity of stiffness but small designe ability, because the nonlinearity is based on the inherent characteristics of mechanism.

(3) Programmable passive compliance[8] is realized by the additional actuators that change the stiffness of material. For example, a tendon mechanism with nonlinear spring[9] cosmists of two redundant actuators that change the internal force of springs. Morita et.al. developed Mechanical Impedance Adjuster (MIA)[10]. These mechanisms realize an arbitrary compliance however the additional actuator occupies volume and weight of the robot.

In this paper, we focus on (2) Passive compliance with high design ability using a simple closed kinematic chain, and a leg mechanism is designed to absorb the impact force on landing motion. The closed kinametic chain consists of four-bar link, and based on the given output force characteristic the link parameters are optimized using the mechanical synthesis method.

2 Nonlinear stiffness mechanism with four-bar link

2.1 Designed mechanism

Figure 3 shows the designed mechanism to absorb the impact force. The leg mechanism consists of two parallelograms that are coupled with 3D kinematic chain (Mechanism g in figure 3) and yields the vertical motion of foot link (link e – f) as shown in figure 4. ℓ_i $(i = 1 \sim 4, \ell)$ mean the length of members, θ_i $(i = 0 \sim 4)$ mean the rotation angle of joints. r is the length of one side of a triangular link and ϕ_2 is one angle. ψ_0 is constant, T – R is a linear spring and (x_R, y_R) is the position of root of spring with its origin at point A. In the initial position $\theta_0 = 0$ and $\theta_1 = \phi_1$ are satisfied, and the spring becomes natural length L_0 which is calculated as;

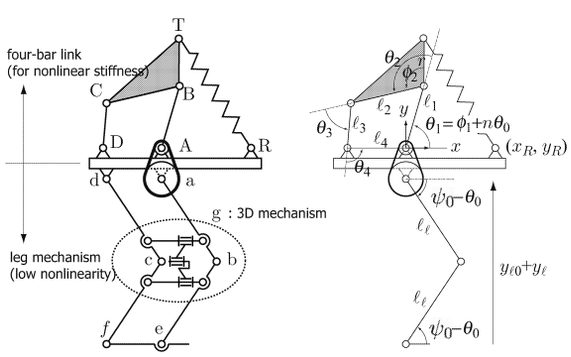

Figure 3: Designed mechanism with four-bar link

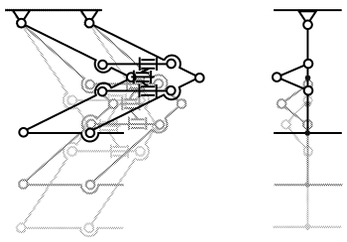

Figure 4: Motion of the leg mechanism

$$L_0 = \sqrt{(x_{T0} - x_R)^2 + (y_{T0} - y_R)^2} \quad (1)$$

$$x_{T0} = \ell_1 \cos\phi_1 + r\cos(\phi_1 + \theta_{20} - \phi_2) \quad (2)$$

$$y_{T0} = \ell_1 \sin\phi_1 + r\sin(\phi_1 + \theta_{20} - \phi_2) \quad (3)$$

where θ_{20} is obtained by the closed kinematic constraints;

$$\sum_{i=1}^{4} \theta_i = 2\pi \quad (4)$$

$$\sum_{i=1}^{4} \ell_i \cos\sum_{j=1}^{i} \theta_j = 0 \quad (5)$$

$$\sum_{i=1}^{4} \ell_i \sin\sum_{j=1}^{i} \theta_j = 0 \quad (6)$$

that form the four-bar link at $\theta_1 = \theta_{10} = \phi_1$. $y_{\ell 0}$ is an initial value of the leg length and calculated by;

$$y_{\ell 0} = -2\ell_\ell \sin\psi_0 \quad (7)$$

The motion of this mechanism is shown in figure 5. The change of y_ℓ yields the rotation of θ_0 and it causes the rotation of θ_1 by the timing belt with its gear ratio 1:n. Because of the nonlinearity of the four-bar link, the length of the spring changes with high nonlinearity, which causes the nonlinear ground force of this mechanism.

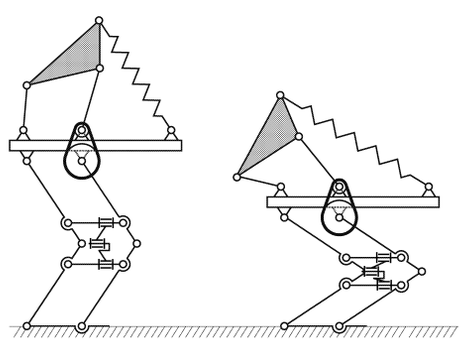

Figure 5: Motion of the designed mechanism

2.2 Ground force calculation

According to the change of y_ℓ, the length of the spring is changed and this mechanism yields the ground force F. In the following, F is calculated. From the kinematics of the leg mechanism, θ_0 is calculated as;

$$\theta_0 = \psi_0 - \sin^{-1}\left(\frac{y_\ell}{2\ell_\ell}\right) \tag{8}$$

The length of the spring L is caliculated by;

$$L = \sqrt{(x_T - x_R)^2 + (y_T - y_R)^2} \tag{9}$$

$$x_T = \ell_1 \cos\theta_1 + r\cos(\theta_1 + \theta_2 - \phi_2) \tag{10}$$

$$y_T = \ell_1 \sin\theta_1 + r\sin(\theta_1 + \theta_2 - \phi_2) \tag{11}$$

The accumulated energy U of the spring is calculated by;

$$U = \frac{1}{2}K(L - L_0)^2 \tag{12}$$

where K is the spring constant. From Castigliano's theorem, the ground force F is obtained by;

$$F = \frac{\partial U}{\partial y_\ell} = \frac{\partial U}{\partial \theta_0}\frac{\partial \theta_0}{\partial y_\ell} \tag{13}$$

and from equation (8),

$$\frac{\partial \theta_0}{\partial y_\ell} = \frac{1}{2\ell_\ell \cos(\psi_0 - \theta_0)} \tag{14}$$

is obtained. On the other hand, from equation (12), the following equation is obtained.

$$\frac{\partial U}{\partial \theta_0} = \frac{\partial U}{\partial \theta_1}\frac{\partial \theta_1}{\partial \theta_0} = K(L - L_0)\frac{\partial L}{\partial \theta_1}\frac{\partial \theta_1}{\partial \theta_0} \tag{15}$$

where

$$\frac{\partial L}{\partial \theta_1} = \frac{(x_T - x_R)\dfrac{\partial x_T}{\partial \theta_1} + (y_T - y_R)\dfrac{\partial y_T}{\partial \theta_1}}{L} \tag{16}$$

$$\frac{\partial \theta_1}{\partial \theta_0} = n \tag{17}$$

$$\frac{\partial x_T}{\partial \theta_1} = -\ell_1 \sin\theta_1 - r\sin(\theta_1 + \theta_2 - \phi_2)\left(1 + \frac{\partial \theta_2}{\partial \theta_1}\right) \tag{18}$$

$$\frac{\partial y_T}{\partial \theta_1} = \ell_1 \cos\theta_1 + r\cos(\theta_1 + \theta_2 - \phi_2)\left(1 + \frac{\partial \theta_2}{\partial \theta_1}\right) \tag{19}$$

and from the closed kinematic constraints in equation (4)∼(6),

$$1 + \frac{\partial \theta_2}{\partial \theta_1} = -\frac{\ell_1 \sin(\theta_2 + \theta_3)}{\ell_2 \sin\theta_3} \tag{20}$$

is obtained. From these equations, once all link parameters are defined, the ground force is calculated as;

$$F = F(y_\ell) \tag{21}$$

3 Mechanical synthesis of four-bar link

Based on the output force obtained in the previous section, the link parameters are obtained using mechanical synthesis method based on the output force.

Suppose that sets of y_ℓ and desired force F_d are given as $(y_\ell^i,\ F_d^i)$ $(i = 1, 2, \cdots)$ and we set the objective function J as;

$$J = \sum_i \left(F_d^i - F(y_\ell^i)\right)^2 \tag{22}$$

And link parameters are optimized so that J is minimized by the least square method. For simplicity, ℓ_ℓ(=20[mm]), ϕ_0(=75[degree]), n(=1.75) and ℓ_4(=10[mm]) are fixed because the change of ℓ_ℓ and ℓ_4 yield a homologous mechanism, ϕ_0 defines the initial position and n cannot be taken an arbitrary value (it is decided by the number of teeth of the timing pulley). The design parameters are the following nine parameters : ℓ_1, ℓ_2, ℓ_3, r, ϕ_2 (link parameters of four-bar link), ϕ_1 (initial value of θ_1), x_R, y_R (root position of the spring) and K (spring constant). By using Newton's method, the design parameter q is renewed as;

$$q \leftarrow q + \frac{\partial J}{\partial q}\delta \tag{23}$$

$$\frac{\partial J}{\partial q} = -2\sum_i \left\{\left(F_d^i - F(y_\ell^i)\right)\frac{\partial F(y_\ell^i)}{\partial q}\right\} \tag{24}$$

where δ is constant. Calculation of $\dfrac{\partial F}{\partial \ell_1}$ is shown in Appendix A for example.

4 Stiffness design and simulation results

4.1 Design of desired force

In this section, a leg mechanism that absorbs the landing force is designed. First, we set the desired force F_d to absorb the landing force and the mechanism is optimized so that it realizes the desired force.

Here we assume that this mechanism with its weight M falls from the height h and collides with the ground with its drop velocity v_M;

$$v_M = \sqrt{2gh} \tag{25}$$

where g is the gravity acceleration. The ground force should satisfy the following conditions.

1. $F_d = 0$ at $y_\ell = 0$ is satisfied because the spring is natural length at $y_\ell = 0$.

2. The stiffness $K_\ell = \partial F_d / \partial y_\ell$ at $y_\ell = 0$ is sufficiently large. It causes the brake for the drop velocity.

3. $F_d = Mg$ at $y_\ell = y_f$ is satisfied, where y_f is the final height of the body.

4. The stiffness at $y_\ell = y_f$ is sufficiently small. It causes the attenuation of the vibration because of the small stiffness.

5. The stiffness in large y_ℓ is sufficiently large. It plays the stopper role.

From these conditions, the desired force F_d is set as shown in figure 6.

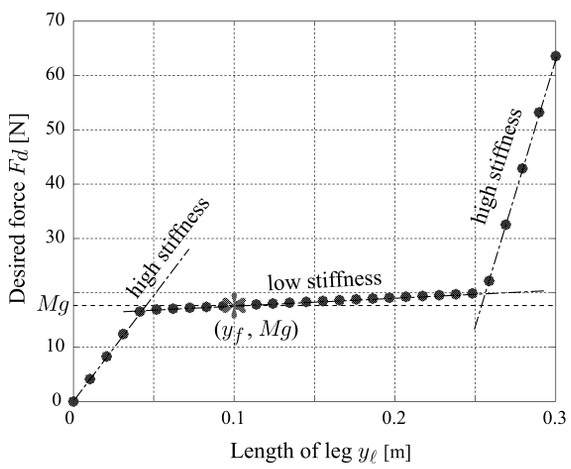

Figure 6: Desired force

4.2 Mechanical synthesis

By setting an appropriate initial value, the design parameters are optimized. The initial configuration and the optimized configuration of the leg mechanism are shown in figure 7, and figure 8

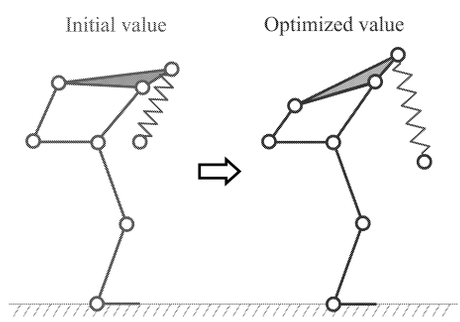

Figure 7: Initial and optimized configuration

shows F of the initial value and the optimized value.

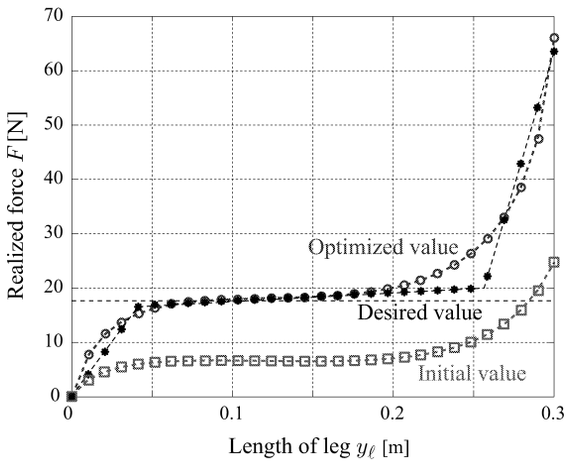

Figure 8: Obtained ground force

4.3 Landing simulation

By using the optimized mechanism, the landing simulation is executed, where the dynamics of the inertia term of members are ignored. The mechanism is approximated by a mass-damper-spring system with the concentrated mass as shown in figure 9. C is a constant viscous coefficient and

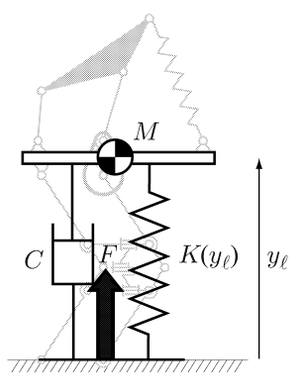

Figure 9: Model of the mechanism

$K(y_\ell)$ is nonlinear stiffness, and they yields the ground force F in equation (21). This mechanism falls from the height $h = 0.05,\ 0.15,\ 0.30$[m] and collides to the ground with its velocity v_M in equation (25). The simulation results are shown in figure 10. The final positions are same because the weight of the robot is same. The transient responses in the simulations are shown in figure $11 \sim 13$. Figure 11 shows the ground force. This figure shows that the nonlinear spring reduces the ground force comparing the linear spring (see $h = 0.05,\ 0.15$[m]), which means the nonlinear spring works as a soft spring. On the other hand, when $h = 0.30$[m], even though the maximum ground force of nonlinear spring is larger than linear spring, the body height is not so much

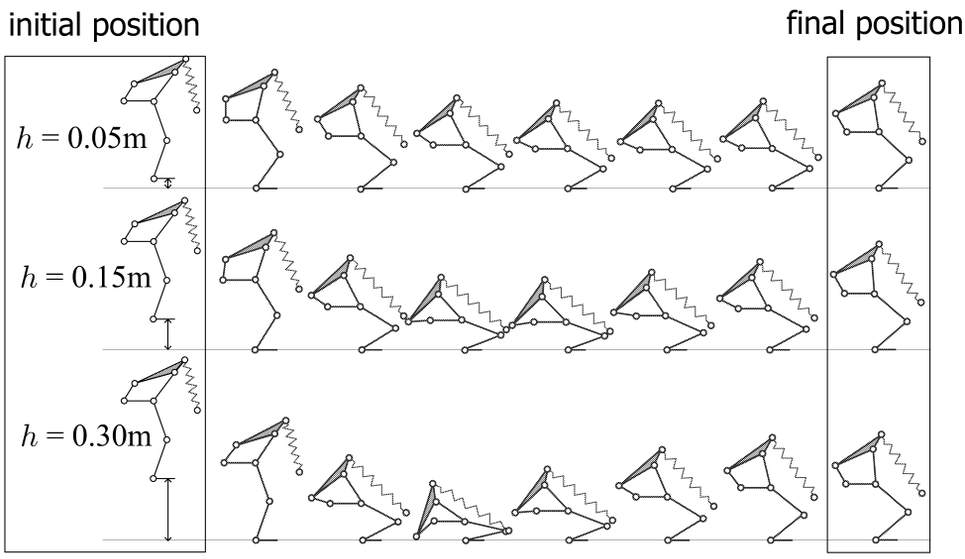

Figure 10: Landing simulations

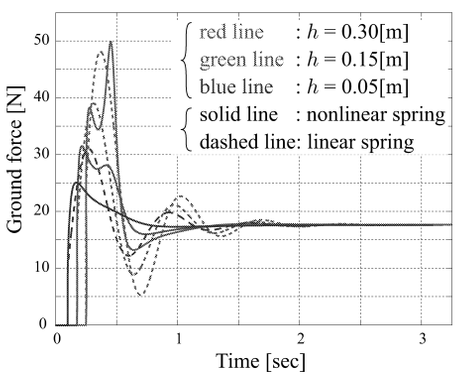

Figure 11: Simulation results of the ground forces

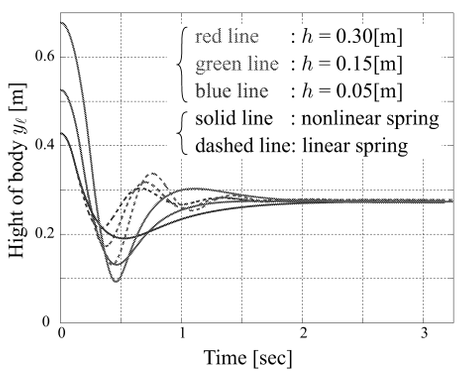

Figure 12: Simulation results of the height of bodies

changed as shown in figure 12, which means the nonlinear spring works as a hard spring. This is because the nonlinear spring has an advantage of the stopper structure. Figure 13 shows the distortion of the spring. The distortions are less than 70% which is smaller than a plastic deformation of the normal spring specification.

5 Conclusions

In this paper, we propose a nonlinearity design method of passive stiffness using closed kinematic chain. The results of this paper are as follows;

1. We propose a leg mechanism that realizes a designable nonlinear stiffness using four-bar link.

2. Optimization method of the link parameters is proposed to realize a specified ground force based on mechanical synthesis.

3. To reduce the impact force of landing, the link parameters are optimized.

4. The effectiveness of the proposed method is evaluated by the landing simulations.

Acknowledgment

This research is supported by the “Motion emergence and mutual progression of robot body and intelligence from the dynamical point of view” under Grants-in-Aid for Scientific Research (Category Encouragement of Young Scientists (A)) of Japan Society for the Promotion of Science.

References

[1] R.P.C.Paul and B.Shimano : Compliance and Control, Proc. of the 1976 Joint Automatic Control Conference, pp.694–699 (1976)

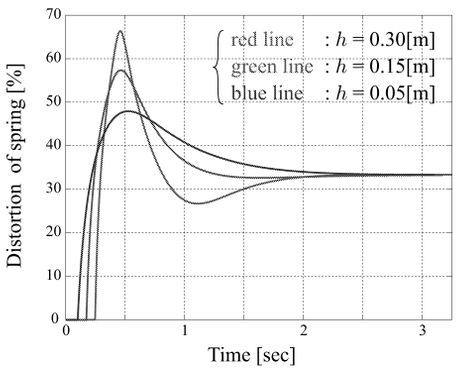

Figure 13: Distortion of the springs

[2] H.Hanafusa and H.Asada : Stable Pretension by a Robot Hand with Elastic Fingers, Proc. of the 7th International Symposium on Industrial Robots, pp.361–368 (1977)

[3] N.Hogan : Mechanical Impedance Control in Assistive Devices and Manipulators, Proc. of the 1980 Joint Automatic Control Conference, pp.TA10-B (1980)

[4] J.K.Salisbury : Active Stiffness Control of a Manipulator in Cartesian Coordinates, Proc. of the IEEE Conference on Decision and Control (1980)

[5] N.Hogan : Impedance Control: An Approach to Manipulation: Part 1∼3, ASME Journal of Dynamic Systems, Measurement and Control, Vol.107, pp.1–24 (1985)

[6] M.Okada and Y.Nakamura: Development of the Cybernetic Shoulder – A Three DOF Mechanism that Imitates Biological Shoulder-Motion –, Proc. of IEEE/RSJ International Conference on Intelligent Robots and Systems , Vol.2, pp.543-548 (1999)

[7] M.Okada and S.Kino: Torque Transmission Mechanism with Nonlinear Passive Stiffness using Mechanical Singularity, Proc. of the IEEE International Conference on Robotics and Automation (ICRA'08), pp.1735-1740, (2008)

[8] K.F.L-Kovitz, J.E.Colgate and S.D.R.Carnes: Design of Components for Programmable Passive Impedance, Proc. of IEEE International Conference on Robotics and Automation, pp.1476–1481 (1991)

[9] H.Kobayashi, K.Hyodo and D.Ogane: On Tendon-Driven Robotic Mechanism with Redundant Tendons, Int. J. of Robotics Research, Vol.17, No.5, pp.561-571 (1998)

[10] T.Morita and S.Sugano: Design and Development of a new Robot Joint using a Mechanical Impedance Adjuster, Proc. of IEEE International Conference on Robotics and Automation, pp.2469-2475 (1995)

Appendix

A Calculation of $\partial F/\partial \ell_1$

From equation (13), the following equation is obtained.

$$\frac{\partial F}{\partial \ell_1} = \frac{\partial}{\partial \ell_1}\left(\frac{\partial U}{\partial y_\ell}\right) = \frac{\partial}{\partial \ell_1}\left(\frac{\partial U}{\partial \theta_1}\frac{\partial \theta_1}{\partial \theta_0}\frac{\partial \theta_0}{\partial y_\ell}\right)$$
$$= \frac{\partial}{\partial \ell_1}\left(2K(L-L_0)\frac{\partial L}{\partial \theta_1}\right)\frac{\partial \theta_1}{\partial \theta_0}\frac{\partial \theta_0}{\partial y_\ell} \quad \text{(A.1)}$$
$$= 2K\left\{\left(\frac{\partial L}{\partial \ell_1} - \frac{\partial L_0}{\partial \ell_1}\right)\frac{\partial L}{\partial \theta_1} + (L-L_0)\frac{\partial}{\partial \ell_1}\left(\frac{\partial L}{\partial \theta_1}\right)\right\}\frac{\partial \theta_1}{\partial \theta_0}\frac{\partial \theta_0}{\partial y_\ell} \quad \text{(A.2)}$$

$$\frac{\partial L}{\partial \ell_1} = \frac{(x_T - x_R)\dfrac{\partial x_T}{\partial \ell_1} + (y_T - y_R)\dfrac{\partial y_T}{\partial \ell_1}}{L} \quad \text{(A.3)}$$

$$\frac{\partial x_T}{\partial \ell_1} = \cos\theta_1 - r\sin(\theta_1+\theta_2-\phi_2)\frac{\partial \theta_2}{\partial \ell_1} \quad \text{(A.4)}$$

$$\frac{\partial y_T}{\partial \ell_1} = \sin\theta_1 + r\cos(\theta_1+\theta_2-\phi_2)\frac{\partial \theta_2}{\partial \ell_1} \quad \text{(A.5)}$$

$$\frac{\partial \theta_2}{\partial \ell_1} = -\frac{\cos(\theta_2+\theta_3)}{\ell_2\sin\theta_3} \quad \text{(A.6)}$$

$$\frac{\partial L_0}{\partial \ell_1} = \left.\frac{\partial L}{\partial \ell_1}\right|_{\theta_1=\phi_1,\theta_2=\theta_{20},\theta_3=\theta_{30},L=L_0} \quad \text{(A.7)}$$

$$\frac{\partial x_{T0}}{\partial \ell_1} = \left.\frac{\partial x_T}{\partial \ell_1}\right|_{\theta_1=\phi_1,\theta_2=\theta_{20},\theta_3=\theta_{30}} \quad \text{(A.8)}$$

$$\frac{\partial y_{T0}}{\partial \ell_1} = \left.\frac{\partial y_T}{\partial \ell_1}\right|_{\theta_1=\phi_1,\theta_2=\theta_{20},\theta_3=\theta_{30}} \quad \text{(A.9)}$$

Here we remark that the change of ℓ_1 causes the change of θ_{20} and θ_3 because of the kinematic constraints of four-bar link. And it yields equation (A.7) ∼ (A.9). Other parameters are calculated as follows:

$$\frac{\partial}{\partial \ell_1}\left(\frac{\partial L}{\partial \theta_1}\right) = \frac{1}{L}\left\{\frac{\partial x_T}{\partial \ell_1}\frac{\partial x_T}{\partial \theta_1} + (x_T - x_R)\frac{\partial}{\partial \ell_1}\left(\frac{\partial x_T}{\partial \theta_1}\right) + \frac{\partial y_T}{\partial \ell_1}\frac{\partial y_T}{\partial \theta_1} + (y_T - y_R)\frac{\partial}{\partial \ell_1}\left(\frac{\partial y_t}{\partial \theta_1}\right)\right\} - \frac{1}{L^2}\left\{(x_T-x_R)\frac{\partial x_T}{\partial \theta_1} + (y_T-y_R)\frac{\partial y_T}{\partial \theta_1}\right\}\frac{\partial L}{\partial \ell_1} \quad \text{(A.10)}$$

$$\frac{\partial}{\partial \ell_1}\left(\frac{\partial x_t}{\partial \theta_1}\right) = -\sin\theta_1 - r\cos(\theta_1+\theta_2-\phi_2)\frac{\partial \theta_2}{\partial \ell_1}\left(1+\frac{\partial \theta_2}{\partial \theta_1}\right) - r\sin(\theta_1+\theta_2-\phi_2)\frac{\partial}{\partial \ell_1}\left(\frac{\partial \theta_2}{\partial \theta_1}\right) \quad \text{(A.11)}$$

$$\frac{\partial}{\partial \ell_1}\left(\frac{\partial y_T}{\partial \theta_1}\right) = \cos\theta_1 - r\sin(\theta_1+\theta_2-\phi_2)\frac{\partial \theta_2}{\partial \ell_1}\left(1+\frac{\partial \theta_2}{\partial \theta_1}\right) + r\cos(\theta_1+\theta_2-\phi_2)\frac{\partial}{\partial \ell_1}\left(\frac{\partial \theta_2}{\partial \theta_1}\right) \quad \text{(A.12)}$$

$$\frac{\partial}{\partial \ell_1}\left(\frac{\partial \theta_2}{\partial \theta_1}\right) = \frac{1}{\ell_2^2\sin^2\theta_3}\left\{\ell_1\ell_2\sin(\theta_2+\theta_3)\cos\theta_3\frac{\partial \theta_3}{\partial \ell_1} - \left\{\sin(\theta_2+\theta_3) + \ell_1\cos(\theta_2+\theta_3)\left(\frac{\partial \theta_2}{\partial \ell_1}+\frac{\partial \theta_3}{\partial \ell_1}\right)\right\}\right\} \quad \text{(A.13)}$$

$$\frac{\partial \theta_3}{\partial \ell_1} = \frac{\cos\theta_1 - \ell_2\sin(\theta_1+\theta_2)\dfrac{\partial \theta_2}{\partial \ell_1}}{\ell_3\sin(\theta_1+\theta_2+\theta_3)} - \frac{\partial \theta_2}{\partial \ell_1} \quad \text{(A.14)}$$